Synchronization and control of coupled Ginzburg-Landau equations using local coupling

Lutz Junge* and Ulrich Parlitz
Drittes Physikalisches Institut, Universität Göttingen, Bürgerstraße 42-44, D-37073 Göttingen, Germany
(Received 22 October 1999)

In this paper we discuss the properties of a recently introduced coupling scheme for spatially extended systems based on local spatially averaged coupling signals [see Z. Tasev *et al.*, Int. J. Bifurcation Chaos Appl. Sci. Eng. (to be published); and L. Junge *et al.*, Int. J. Bifurcation Chaos Appl. Sci. Eng. **9**, 2265 (1999)]. Using the Ginzburg-Landau model, we performed an extensive numerical examination of this coupling scheme, i.e., a complete scan through the relevant coupling parameters. Furthermore, we demonstrate suppression and control of spatiotemporal chaos, e.g., stabilizing the homogeneous steady state and spatially localized control. As an application all model parameters of the Ginzburg-Landau equation are estimated given only the local information of the system.

PACS number(s): 05.45.Xt, 05.45.Gg, 05.45.Jn

I. INTRODUCTION

Synchronization phenomena are of fundamental importance in many physical, biological, and technical systems. In particular, synchronization of chaotic dynamics [1] has attracted much attention during the last few years because of its role in understanding the basic features of coupled nonlinear systems and in view of potential applications in communication systems, time series analysis, and modeling [2]. Different coupling schemes have been proposed in order to achieve synchronization in particular for unidirectionally coupled systems [1]. Recently, synchronization and control of spatially extended systems such as coupled map lattices (CML's) [3], arrays of coupled oscillators [4], or partial differential equations [5] have gained much interest. Most of the studies focused on coupled map lattices, which are the simplest models for spatiotemporal chaos and are the first step when exploring spatially extended systems. CML's are discrete in time and space and the individual maps are usually diffusively coupled in space, e.g., with nearest neighbor coupling. Diffusively coupled ordinary differential equations (CODE's) are the next step (continuous in time and discrete in space) [4]. A widely used controling technique for both system classes is the so-called ''pinning control'' [3] which affects single cells, e.g., maps or ODE's, or in the case of synchronization, connects pairs of single cells of the two systems. When we now consider the next step and go to systems with continuous space variables, e.g., partial differential equations (PDE's), we run into trouble. The reason is that we no longer have single cells to control or to connect. Instead we now have a continuum and the pinning control technique which acts on points in space is no longer applicable [6]. Therefore, we use in this paper a recently introduced coupling scheme for PDE's [7,8] based on local spatial averaged coupling signals (sensors), which are a model for typical experimental sensors and actuators.

The sensor coupling scheme is introduced in the next section. In Sec. III we present the results of a detailed numerical examination of the synchronization of two coupled Ginzburg-Landau equations using the sensor coupling and discuss the influence of relevant coupling parameters. In Sec. IV the coupling scheme is used for controlling purposes and in Sec. V we demonstrate that distinct *local* regions of the PDE's can be synchronized and controlled, while the rest of the space remains unaffected. As an application of the sensor coupling scheme we estimate all model parameters of a PDE in Sec. VI.

II. SYNCHRONIZATION OF SPATIALLY EXTENDED SYSTEMS

In the past decade, synchronization of dynamical systems has attracted much interest and various definitions and types of synchronization were proposed, e.g., identical [1], generalized [9], lag and phase synchronization [10]. In this paper, we restrict ourselves to *identical synchronization* where the two coupled dynamical systems are exactly of the same type and given by a partial differential equation of the form

$$\frac{\partial u}{\partial t} = F\left(u, \frac{\partial u}{\partial x}, \frac{\partial^2 u}{\partial x^2}, \dots \right), \quad x \in [0,L] \tag{1}$$

with spatial length L [11]. Usually one speaks of synchronization of two coupled dynamical systems when the temporal evolution of their states coincides after some initial transient. If both coupled systems are of the same type *identical synchronization* may occur where the states $u(t)$ and $v(t)$ of drive and response, respectively, converge to the same values (i.e. $\|u(t)-v(t)\| \to 0$ for $t \to \infty$). Note, that when we are looking at spatially extended systems like PDE's, the states $u(x,t)$ and $v(x,t)$ are continuous functions of the spatial variable(s) and the state space is infinite dimensional. In this case the above definition reads as follows: Two spatially extended systems are called identically synchronized, if their states converge to each other in the whole spatial domain, i.e., $\forall x \in [0,L]: \lim_{t\to\infty} \|u(x,t)-v(x,t)\| = 0$.

For $x \in \mathbb{Z}$ and $t \in \mathbb{Z}$ this is the definition of synchronization of CML's, for $x \in \mathbb{Z}$ and $t \in \mathbb{R}$ for CODE's and for $x,t \in \mathbb{R}$ for PDE's. As in the case of coupled oscillators there exists an invariant manifold $u(x) \equiv v(x)$ (also called synchronization manifold), whose stability properties determine the occur-

*Electronic address: L.Junge@dpi.physik.uni-goettingen.de

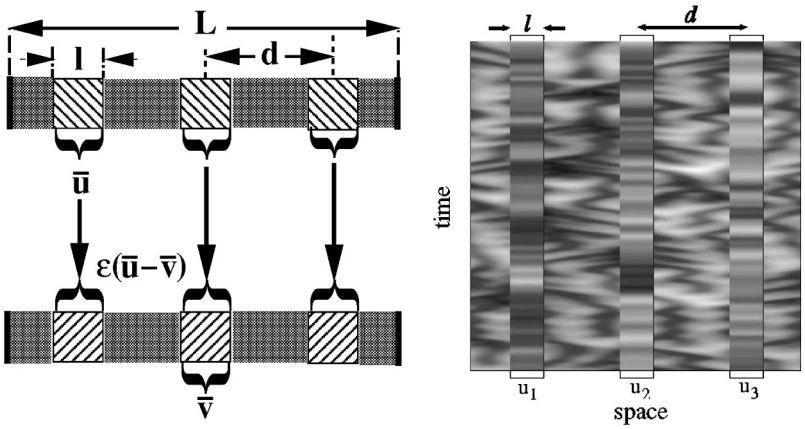

FIG. 1. Left: Principle of the sensor coupling scheme. Right: Visualization of three sensor time series (plotted overlayed) measured from spatiotemporal chaos.

rence of stable (high quality) synchronization [12]. This manifold is asymptotically stable and high quality synchronization occurs if the transverse subsystem $w_\perp(x,t) = \frac{1}{2}[u(x,t)-v(x,t)]$ has an asymptotically stable fixed point at zero. Indeed, all techniques [1] for verifying synchronization, e.g., *necessary* criteria like negative conditional Lyapunov exponents or *sufficient* criteria [12] like Lyapunov functions and stability of invariant sets, can be generalized and in principle be applied to these systems, too.

But the particular coupling techniques often are difficult to generalize for PDE's in a straightforward way, because this would imply that one has to couple in the whole spatial domain [13] or in points [3,5,14], which may be impractical in experiments. The *sensor* coupling scheme, introduced in Refs. [7,8], generalizes the pinning coupling scheme to systems with continuous space variables. The idea is that typical experimental measuring devices have a finite resolution l and measure local spatial averages of some spatial observable. According to Refs. [7,8] we want to call these elements *sensors* that measure scalar time series of the form

$$\overline{u}_n(t) = \frac{1}{l}\int_{nd-l/2}^{nd+l/2} u(t)dx, \quad n=1,\ldots,N, \tag{2}$$

which represent average values of spatial intervals of width l. Figure 1(b) shows a spatiotemporal chaotic dynamics where the amplitude information is color coded. We have measured with three sensors yielding three scalar signals which are plotted overlayed on the original dynamics. One sees that we cannot resolve all fine detail in space anymore, but we have now, due to our finite resolution, only some averaged information about the local dynamics from parts of the system. However, as we shall demonstrate in the following, this is for properly chosen coupling parameters enough to completely synchronize this system with another (identical) system using the sensor time series as coupling signals.

Because of the exponential decrease of spatial correlations in extended chaotic systems, we need for this coupling technique several but a finite number N of coupling signals that contain all the necessary information to reconstruct the whole state in the synchronization process. An equidistant arrangement of N sensors with distance $d=L/N$ turns out to be nearly optimal (for periodic boundary conditions) for this coupling scheme [8]. Now we have to choose a coupling term that will be applied locally with each sensor signal as driving force. We use throughout this paper a unidirectional dissipative coupling, but we want to stress that other coupling terms should work well, too. To implement this coupling we have to measure in the driven system N sensor signals at the same positions and apply the dissipative coupling term with coupling strength ϵ

$$f(\overline{u}_n,\overline{v}_n) = \begin{cases} \epsilon(\overline{u}_n-\overline{v}_n), & nd-l/2 \leqslant x \leqslant nd+l/2 \\ 0, & \text{elsewhere} \end{cases} \tag{3}$$

at each sensor position $n=1,\ldots,N$, respectively. Figure 1(a) shows the principle of the sensor coupling scheme and illustrates where we place the sensors and apply the local dissipative coupling forces.

As an example we examine in this paper the one-dimensional complex Ginzburg-Landau equation (GLE) [15,16]

$$\frac{\partial u}{\partial t} = \mu u - (1-i\alpha)|u|^2 u + (1+i\beta)\Delta u, \quad u \in [0,L] \tag{4}$$

with periodic boundary conditions. This equation possesses uniform traveling wave solutions, which are all unstable for parameter values of α and β with $1-\alpha\beta<0$ where different types of turbulence occur. In this paper we examine two parameter sets, $\mu=1.0$, $\alpha=2.0$, and $\beta=0.7$ corresponding to phase turbulence [see Fig. 2(a)] and $\mu=1.0$, $\alpha=2.0$, $\beta=1.2$, which yields defect turbulence [see Fig. 2(b)]. For synchronization purposes we apply to an identical copy of Eq. (4) at N locations coupling terms (3) using sensors of width l. Note that this is a local control technique and the driven system

$$\frac{\partial v}{\partial t} = \mu v - (1-i\alpha)|v|^2 v + (1+i\beta)\Delta v + f(\overline{u}_n,\overline{v}_n) \tag{5}$$

can evolve between the sensor locations freely in time. In Fig. 3 we use $N=15$ equally spaced sensors with width $l=3$ and coupling strength $\varepsilon=0.2$ to synchronize two GLE's with length $L=100$ in the phase turbulent regime.

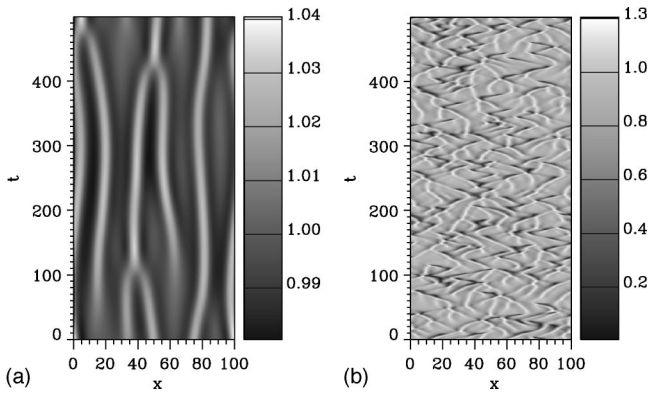

FIG. 2. Dynamical regimes of the Ginzburg-Landau equation (4). (a) Phase turbulence. (b) Defect turbulence, amplitudes are gray scaled.

Figure 3(a) shows the dynamics of the driving system and in Fig. 3(b) the evolution of the response system is plotted. At $t=170$ the coupling is switched on and the response system converges quickly to the synchronized state. At the beginning of the coupling the perturbation introduced through the controllers induces a periodic pattern, which decays very fast in favor of the dynamics of the synchronized state. In the next section we shall study this coupling scheme and the involved parameters in more detail.

III. INTERDEPENDENCE OF THE COUPLING PARAMETERS OF THE SENSOR COUPLING

In this section we discuss the results from an intensive numerical investigation of the properties of the sensor coupling scheme using the one-dimensional GLE. In particular, we shall discuss the relation and interdependence of the three coupling parameters N, l, and ϵ. For solving the PDE's we used an implicit Crank-Nichelson discretization scheme [17] which is second order in space, first order in time, and unconditionally stable. For consistency, all simulations were performed with a time step of 0.01 and a grid of 2 points per unit length of the PDE. We checked the calculations for finer resolutions in space and time and found qualitatively and quantitatively good agreement.

The GLE shows extensive chaos which means that extensive quantities like the attractor dimension are growing lin-

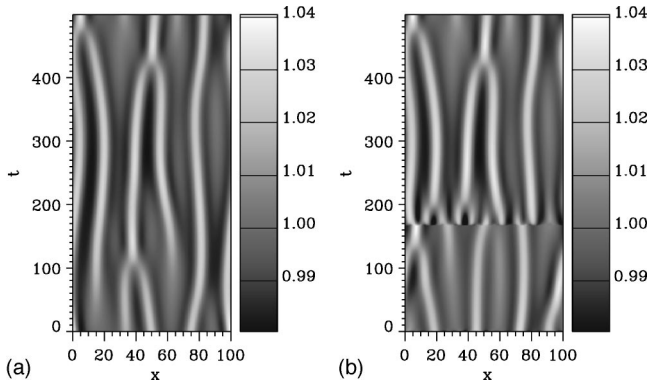

FIG. 3. Synchronization of two coupled GLE's in the phase turbulent regime. (a) Drive system. (b) Response system driven by $N=15$ sensors with width $l=3$ and coupling strength $\epsilon=0.2$.

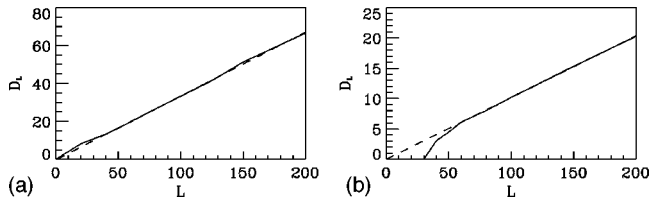

FIG. 4. Lyapunov dimension D_L vs the system length L for defect turbulence [(a) $\mu=1.0,\alpha=2.0,\beta=1.2$] and phase turbulence [(b) $\mu=1.0,\alpha=2.0,\beta=0.7$].

early with the system size. We checked this numerically and have computed the Lyapunov dimension for several lengths [18].

In Fig. 4 the Lyapunov dimension is plotted vs the length L in the two examined dynamical regimes (see. Fig. 2). The Lyapunov dimension D_L shows an excellent linear scaling with the length L for phase and defect turbulence, which confirms the results of Keefe [16]. Making a least squares fit of the slopes we obtain the following relations, $D_L \sim 0.332L$ for defect turbulence and $D_L \sim 0.102L$ for phase turbulence. The higher slope for the defect turbulent regime reflects the more erratic and complex behavior of the dynamics in this regime. In the rest of this section, we want to examine the synchronization of defect turbulence in more detail.

In experiments one often wants to use as few controllers as possible. Therefore, we computed the minimal number N of sensors needed to synchronize the two systems for several configurations of the coupling parameters. In the following this quantity will serve as an indicator for the performance of the used coupling configuration.

Figure 5 shows the scaling of the minimal number of needed sensors N with the system length L for fixed width l and different values of the coupling strength ε of the local coupling term. In the left plot the width l is fixed to 0.5 and in the right plot $l=3.0$. Each line corresponds to a specific coupling strength ε which increases from top $\varepsilon=0.5$ to bottom $\varepsilon=4.0$. Note that the minimal number of sensors N needed for synchronization scales linearly with the system length L, which is valid for all combinations of l and ε yielding synchronization. In other words, the distance between two sensors remains constant when one increases the length L of the system. This distance is of the same order as the correlation length of the dynamics. The reason that we do not have to couple in the whole spatial domain is the fact that

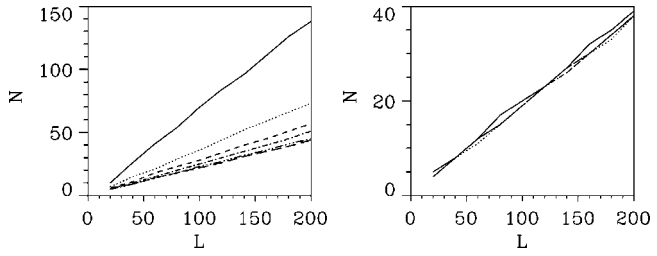

FIG. 5. Minimal number N of coupling signals needed for synchronization vs the spatial length L for fixed width l of the sensors. Left: $l=0.5$ and right $l=3.0$. The coupling strength ε increases from top to bottom $\varepsilon=0.5,1.0,1.5,2.0,3.0,4.0$.

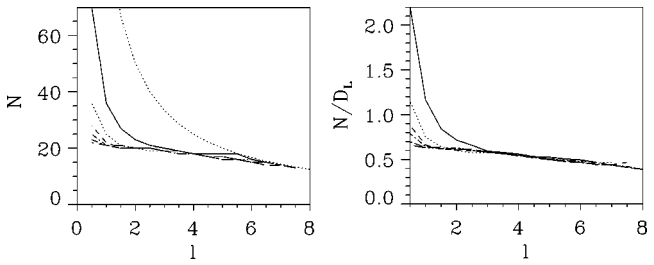

FIG. 6. The left figure shows the minimal number N of sensors needed for synchronization vs the width l of the sensors for a fixed system length $L=100$. The right plot shows the number N of sensors needed for synchronization normalized to the Lyapunov dimension D_L vs the width l. The coupling strength ε increases from top to bottom $\varepsilon=0.5,1.0,1.5,2.0,3.0,4.0$. The dotted line in the left plot indicates the border where the sensors begin to overlap.

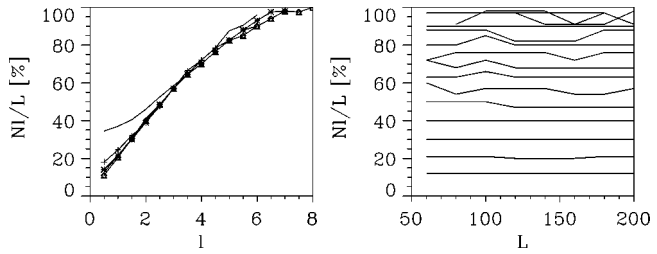

FIG. 7. Percentage of the system size L covered by the controllers vs l and L: Left: Nl/L vs l for $L=200$ and $\varepsilon=0.5,1.0,1.5,2.0,3.0,4.0$ (from bottom to top). Right: Nl/L vs L for $\varepsilon=2.0$ and $l=0.5,\ldots,8.0$ (from bottom to top).

the uncoupled areas are correlated with the coupled areas in their neighborhood and they receive the information about the drive dynamics due to the internal spatial diffusion of the system. In the left plot of Fig. 5 we used $l=0.5$, which is one grid point per controller and means coupling in pinning points in the used spatial resolution of the numerical integration scheme. The stronger the coupling strength ε the less coupling signals we need to obtain synchronization. This is what one might expect: stronger coupling leads to better performance. In the right plot we used the spatially extended sensor signals of width $l=3.0$ and we find that the number of sensor signals N seems to be independent of ε and we need fewer controllers than in the left plot. The explanation of this phenomena is again that the uncoupled areas receive the information from the neighboring coupled areas due to internal diffusion. When we use very small sensors we have to apply a strong coupling force to transport the local drive information to the uncoupled areas between the sensor positions. But when using spatially extended sensors it is not necessary to apply strong coupling because the uncoupled areas are much smaller than in the case of coupling with pinnings. On the other hand, because of using local spatially averaged coupling signals, we do not have to transmit more information to achieve this. The left plot in Fig. 6 shows the dependence of N on the width l for a fixed system length of $L=100$, the coupling strength ε increases from top to bottom. For pinning coupling ($l=0.5$ in our spatial grid) we have to apply strong forcing to yield good performance (in the sense of using fewer coupling signals or controllers). By increasing the width l of the sensor signals we find good performance even for weak coupling strengths. Using very wide sensors is slightly better than intermediate values of the width l, but then we come close to the (dotted) line where the sensors start to overlap which means that the controllers cover the whole system length L. To show that this behavior of the coupling scheme is quite general, at least for the GLE, we consider in the right part of Fig. 6 a quantity which is independent of the system length L. Because the number N of sensors needed to obtain synchronization behaves like an extensive quantity, we can eliminate the system length L by calculating the slopes m of Fig. 5. A small slope indicates good performance while a greater slope means that we have to use more controllers per unit length of the system to achieve synchronization. Since the Lyapunov dimension D_L also depends linearly on the system size L, the slope $m=N/L$ is equivalent to N/D_L. With the relations $D_L\approx 0.331L$ and $N\approx mL$ [19], we can convert the slopes m to $N/D_L\approx m/0.331$. This quantity is plotted in the right plot of Fig. 6.

The quantity N/D_L is independent of the system length L and is a measure for the minimal number of controllers per attractor dimension needed for synchronization with this coupling. This allows us to study the benefit of using spatially extended sensors in a compact and systematic way. The right plot of Fig. 6 indicates that the efforts necessary for synchronizing two coupled GLE's (4) and (5) with sensor coupling depend only on the dimensionality of the underlying chaotic attractor. To synchronize the two coupled GLE's [Eqs. (4) and (5)] it is sufficient to use about 0.5 controllers per attractor dimension. One needs the fewest coupling signals when coupling with sensors which possess a large width l. Therefore, from a practical point of view, the sensor coupling is superior to the pinning coupling technique.

Because of the use of spatially extended sensors one may ask how much area is used by the controllers. This problem is addressed in Fig. 7 where the percentage of the area in space covered by the sensors and controllers Nl/L is plotted vs the width l and the system size L, respectively. The left plot of Fig. 7 shows clearly that the price one has to pay for transmitting fewer sensor signals by using controllers with greater width l (see Fig. 6) is the larger area one has to influence. When one is transmitting the minimum information by using the largest possible width l one has to couple in the whole spatial domain. Therefore, the loss of information through the local averaging process and by using fewer coupling signals is compensated through a larger size of the coupled areas. The left plot of Fig. 7 shows that this effect is independent of the system size L. In the diagram on the right-hand side of Fig. 7, Nl/L is plotted vs the system size L for different values of the width l. The percentage of the area used for coupling is for a fixed coupling configuration independent of the system length [20]. This confirms our statement above that the distance between the controllers remains constant for fixed l and ε and therefore the covered area, too.

IV. STABILIZING THE HOMOGENEOUS STEADY STATE

The sensor coupling technique can also be applied to suppress spatiotemporal chaos. To demonstrate this, we have stabilized the homogeneous steady state $u\equiv 0$ of Eq. (4). This state is a solution of Eq. (4) and is highly unstable. To

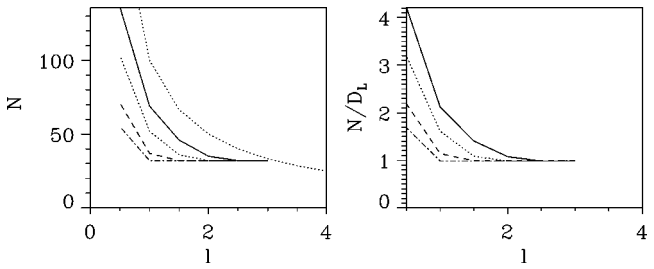

FIG. 8. Number N of sensors needed for stabilizing the homogeneous steady state $u \equiv 0$ vs the width l for a fixed system length $L=100$ (left) and normalized by the Lyapunov dimension D_L (right). The coupling strength ε increases from top to bottom ($\varepsilon = 1.5, 2.0, 3.0, 4.0$).

do this we used $u(x)=0$ as a driving signal for the sensors, i.e., we try to synchronize the driven system with the zero solution $u \equiv 0$. Again we have scanned the coupling parameters and the results are presented in Fig. 8. The plots are similar to Fig. 6. The left diagram in Fig. 8 shows the number N of sensors needed for stabilization of $u \equiv 0$ vs the width l for a fixed system length $L=100$. In the right plot the quantity N normalized by the Lyapunov dimension D_L of the unperturbed dynamics is given in dependence on the width l. The relations between the coupling parameters remain qualitively the same compared to the synchronization case, but now one has to use more controllers to achieve the control goal. The quotient N/D_L is again independent of the system size L. This quantity is plotted vs l in the right-hand side of Fig. 8. One may conclude that at least one sensor controller per attractor dimension is necessary, which is approximatively twice that in the synchronization case.

This is intuitively clear when one remembers that the state $u \equiv 0$ is not an attractive set in phase space while the original attractor is a stable solution of Eq. (4). It is thus not surprising that the controllers have to be closer to each other. For widths $l > 3$ we were not able to stabilize the homogeneous steady state $u \equiv 0$ and turbulence or stationary solutions occur between the controllers dependending on the coupling strength ε and the number of controllers N.

V. LOCALIZED SYNCHRONIZATION AND CONTROL

In the preceding sections we have applied the sensor coupling scheme globally, which means that our goal was to control/synchronize the driven system on the whole spatial axis. In the following we demonstrate synchronization and control of parts on the spatial domain. The sensor coupling is a local control technique and we have argued above that the performance of the coupling scheme depends only on the distance between neighboring controllers. Therefore it is not surprising that it is also possible to achieve the desired goal dynamics only in local regions. In Fig. 9 we suppress chaos only in two regions. To do this, we have arranged in two areas four controllers with width $l=2.0$ and a coupling strength $\varepsilon=2.0$, respectively. The small rectangles in Fig. 9 indicate the position and width of the controllers. The figure shows that chaos is successfully suppressed in the two areas. Near the border of the sensors the chaotic dynamics is not totally suppressed and we observe slight fluctuations around zero but in the middle of the two regions the amplitude vanishes completely. The rest of the system remains in the defect turbulent regime.

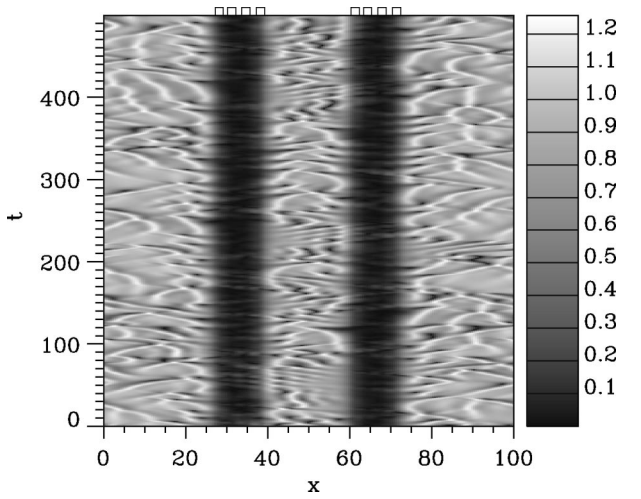

FIG. 9. Local suppression of chaos using two areas with four controllers of width $l=2.0$ and coupling strength $\varepsilon=2.0$, respectively. The small rectangles on top of the diagram indicate the position and the width of the sensors. The figure shows the amplitude dynamics of the controlled system v. The system length was $L=100$ and the parameters $\mu=1.0, \alpha=2.0, \beta=1.2$ lead to defect turbulence.

In Fig. 10 we tried to synchronize the two systems in two regions using six controllers with width $l=2.0$ and a coupling strength $\varepsilon=2.0$, respectively. The upper plot shows the amplitude dynamic of the driven system where again the positions of the controllers are indicated through small rectangles. To verify local synchronization, the lower plot of Fig. 10 shows the local synchronization error $e(x,t) = |u(x,t) - v(x,t)|$. In the coupled regions we observe stable synchronization with only slight fluctuation around the synchronized state at the borders of the controlled areas.

VI. PARAMETER ESTIMATION OF SPATIALLY EXTENDED SYSTEMS

As an application of the sensor coupling scheme we estimate the model parameters of the GLE using a method based on chaos synchronization. This method was demonstrated by several authors [2] to work well for coupled maps and ODE's even with experimental data. The use of synchronization has the advantage that only the parameter vector **p** has to be estimated and not the whole state of the driving system. This gives a drastic reduction in the complexity of the problem, in particular in the case of spatially extended systems. Suppose we have a dynamical system which is well modeled through a map, ODE, or in our case through a PDE, e.g.,

$$\frac{\partial u}{\partial t} = F\left(u, \frac{\partial u}{\partial x}, \frac{\partial^2 u}{\partial x^2}, \ldots; \mathbf{p} \right), \quad x \in [0, L]. \tag{6}$$

Furthermore, we assume that the system can be identically synchronized with a computer model driven by the measured sensor signals $s_i = h_i(u), i = 1, \ldots, N$, if we know the correct parameter vector **p**. The strategy to find this set of correct parameters is the following. We choose an initial guess of

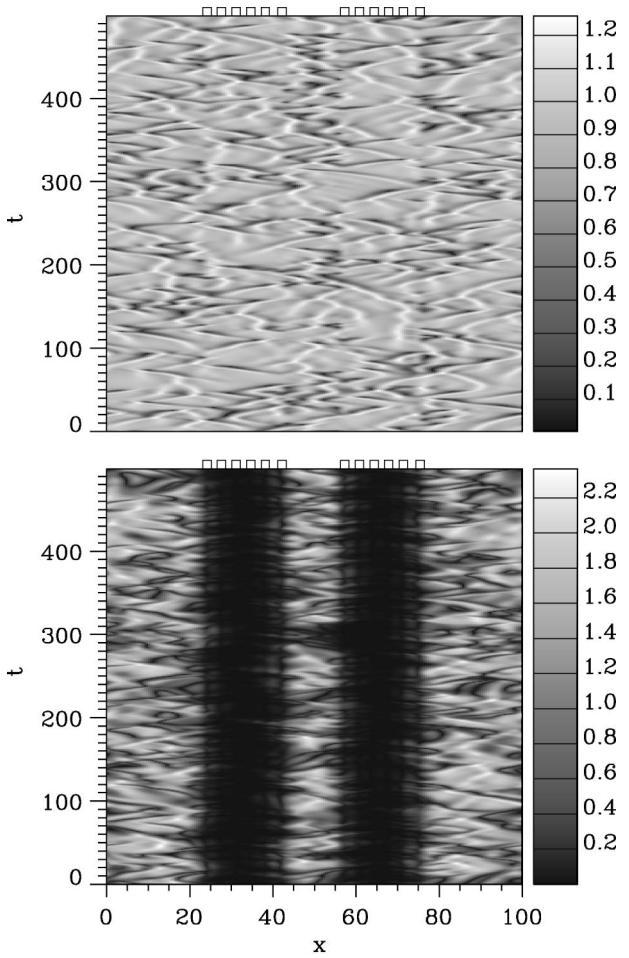

FIG. 10. Local synchronization of chaos using two areas with six controllers of width $l=2.0$ and coupling strength $\varepsilon=2.0$, respectively. The small rectangles indicate the position and the width of the sensors. The system length was $L=100$ and the parameters $\mu=1.0,\alpha=2.0,\beta=1.2$ result in defect turbulence. Top: amplitude dynamics of the response system v. Bottom: synchronization error $|u-v|$.

the parameter vector $\mathbf{p_0}$ and if this choice is not too bad a more sophisticated form of synchronization called generalized synchronization [9] occurs. The driving system determines the dynamics of the driven system still in a unique manner despite the parameter difference between the two systems. The attractors of drive and response are not identical copies of each other, but there still exists a relation between them. We can use this behavior to estimate the unknown parameters $\mathbf{p}$ of our model by varying $\mathbf{p}$ as long as the synchronization error goes to zero which means that the systems synchronize perfectly and we have found the correct parameter vector $\mathbf{p}$ of the driving system.

Generalized synchronization [9] ensures that the synchronization error is a smooth function of $\mathbf{p}$ and simulations indicate that this is valid in a large area of the parameter space [2]. The strategy for parameter finding in Ref. [2] was the minimization of the over M time steps averaged synchronization error $E(\mathbf{p})=\sqrt{1/M\Sigma_{n,i=1}^{M,N}[\overline{u_i^n}-\overline{v_i^n}]^2}\geqslant 0$ where $\overline{u_i^n}$ and $\overline{v_i^n}$ denote the measured sensor signals at position i at the time n. In this paper we want to use another strategy. We compute the synchronization errors of the sensors at some

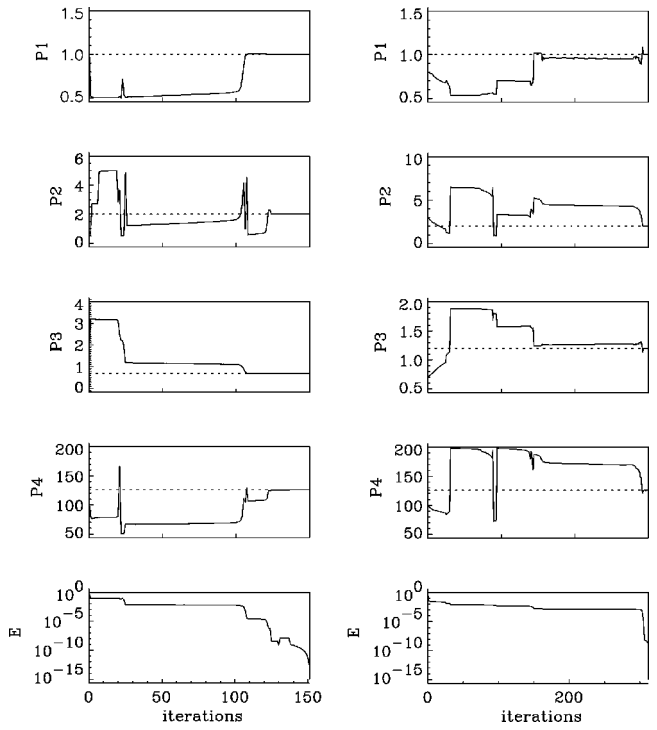

FIG. 11. Convergence of the estimated parameter, the dotted lines show the true parameter values. Left: phase turbulence $P_3=0.7$. Right: defect turbulence $P_3=1.2$.

time T, e.g., $e_i(T;\mathbf{p})=\overline{u_i}(T)-\overline{v_i}(T)$. From the N measured sensor signals we build the error function

$$e(\mathbf{p})=\max\left(\left|\sum_{i=1}^{N}[(\overline{u_i}-\overline{v_i})>0]\right|,\left|\sum_{i=1}^{N}[(\overline{u_i}-\overline{v_i})<0]\right|\right) \tag{7}$$

and determine the roots of $e(\mathbf{p})$ using a simple damped Newton method [17]. In this error function (7) we have summed over all sensor errors $e_i=\overline{u_i}-\overline{v_i}$ which are greater (less) than zero and took the maximum of the absolute values of the two sums as synchronization error. The error function (7) is somewhat sophisticated, but since we synchronize the measured sensor signals with a computer model we can easily compute any complicated cost function. The advantage and motivation of Eq. (7) is the combination of all local synchronization errors into one quantity and the fact that the local errors $e_i(t)$ cannot cancel each other. For the parameter estimation we introduced in Eq. (4) additional parameters including the spatial length $L=p_4$

$$\frac{\partial u}{\partial t}=p_1u-(1-ip_2)|u|^2u+(1+ip_3)\Delta u,\quad x\in[0,p_4]. \tag{8}$$

The PDE was solved again by an implicit scheme but now with a finer resolution of 1000 grid points. We have estimated the parameters of the GLE (8) for two parameter sets. The first set $p_1=1.0,p_2=2.0,p_3=0.7,p_4=L=40\pi$ yields phase turbulent dynamics. To synchronize the two systems we used $N=99$ sensor signals with width $l=0.5$ for the cou-

pling. In the defect turbulent regime $p_1=1.0, p_2=2.0, p_3=1.2, p_4=L=40\pi$ we used $N=33$ sensors with width $l=3.5$. Figure 11 shows the evolution of the parameters during the estimation procedure, phase turbulence (left column) and defect tutbulence (right column). In both regimes all parameters including the spatial length $p_4=L$ are estimated correctly. This shows that even in high-dimensional systems ($D_L \approx 13$ for phase turbulence and $D_L \approx 40$ for defect turbulence) synchronization based parameter estimation methods can be applied succesfully. Note that for phase turbulence coupling in pinning points $l=0.5$ (one spatial grid point in the numerical integration scheme) is used and we needed more coupling signals compared to defect turbulence where wide sensors $l=3.5$ were applied. This shows again the better performance of spatially extended coupling devices. The results are robust with respect to small additional noise on the sensor signals. A more detailed discussion of the performance of synchronization based parameter estimation algorithms with noisy coupling signals can be found in Ref. [21] where the authors examined different low-dimensional systems and a high-dimensional hyperchaotic Rössler type oscillator.

VII. CONCLUSION

In this paper we have examined synchronization and control of continuous spatially extended systems (here the Ginzburg-Landau equation) using locally averaged coupling signals. The number of coupling signals needed for synchronization scales linearly with the system length and the Lyapunov dimension, respectively. Using spatially extended sensors results in a significant reduction of the minimal number of coupling signals. The coupling scheme was applied succesfully for global and local synchronization and control purposes. As an application we used this scheme for estimating the parameters of a PDE from time-series.

ACKNOWLEDGMENTS

We thank L. Kocarev, Z. Tasev, and the members of the nonlinear dynamics group of the Third Physical Institute for stimulating discussions on chaos synchronization, and the DFG (Grant No. Pa 643/1-1) and W. Lauterborn for support.

[1] H. Fujisaka and T. Yamada, Prog. Theor. Phys. **69**, 32 (1983); L. Pecora and T. Carroll, Phys. Rev. Lett. **64**, 821 (1990); L. Kocarev and U. Parlitz, *ibid.* **74**, 5028 (1995); U. Parlitz, L. Kocarev, T. Stojanovski, and H. Preckel, Phys. Rev. E **53**, 4351 (1996); N. Rulkov, Chaos **6**, 262 (1996); U. Parlitz, L. Kocarev, T. Stojanovski, and L. Junge, Physica D **109**, 139 (1997).

[2] R. Brown, N.F. Rulkov, and E.R. Tracy, Phys. Rev. E **49**, 3784 (1994); R. Caponetto, L. Fortuna, G. Manganaro, and M. Xibilia, Proc. SPIE **2612**, 48 (1995); H. Dedieu and M. Ogorzalek, *ibid.* **2612**, 148 (1995); L. Parlitz, L. Junge, and L. Kocarev, Phys. Rev. E **54**, 6253 (1996).

[3] G. Hu and Z. Qu, Phys. Rev. Lett. **72**, 68 (1994); R.O. Grigoriev, M.C. Cross, and H.G. Schuster, *ibid.* **79**, 2795 (1997).

[4] L. Kocarev and U. Parlitz, Phys. Rev. Lett. **77**, 2206 (1996).

[5] L. Kocarev, Z. Tasev, T. Stojanovski, and U. Parlitz, Chaos **7**, 635 (1997); L. Kocarev, Z. Tasev, and U. Parlitz, Phys. Rev. Lett. **79**, 51 (1997); S. Boccaletti, J. Bragard, and F.T. Arecchi, Phys. Rev. E **59**, 6574 (1999).

[6] We want to remark that the numerical solution of PDE's often yields a CML and one might believe that the pinning schemes can be applied to this numerical CML. But this is possible then only due to the numerical discretization and there is no physical justification for this. Moreover, the pinning coupling will depend on the discretization scheme, grid size, etc. The coupling with local spatial averages (sensors) introduced in Refs. [7,8] does not suffer from such artifacts.

[7] Z. Tasev, L. Junge, U. Parlitz, and L. Kocarev, Int. J. Bifuraction Chaos, Appl. Sci. Eng. (to be published).

[8] L. Junge, U. Parlitz, Z. Tasev, and L. Kocarev, Int. J. Bifuraction Chaos Appl. Sci. Eng. **9**, 2265 (1999).

[9] N. Rulkov, M. Sushchik, L. Tsimring, and H. Abarbanel, Phys. Rev. E **51**, 980 (1995); L. Kocarev and U. Parlitz, Phys. Rev. Lett. **76**, 1816 (1996).

[10] M.G. Rosenblum, A. Pikovsky, and J. Kurths, Phys. Rev. Lett. **76**, 1804 (1996); U. Parlitz, L. Junge, W. Lauterborn, and L. Kocarev, Phys. Rev. E **54**, 2115 (1996); G. Osipov, A. Pikovsky, M. Rosenblum, and J. Kurths, *ibid.* **55**, 2353 (1997); M.G. Rosenblum, A.S. Pikovsky, and J. Kurths, Phys. Rev. Lett. **78**, 4193 (1997).

[11] In this paper we restrict ourselves to one-dimensional PDE's, but the coupling scheme [7,8] introduced below can also be applied to higher dimensional PDE's.

[12] D. Gauthier and J. Bienfang, Phys. Rev. Lett. **77**, 1751 (1996).

[13] M. Sushchik, Ph.D. dissertation, University of Californinia, San Diego, 1996.

[14] N. Parekh, S. Parthasarathy, and S. Sinha, Phys. Rev. Lett. **81**, 1401 (1998).

[15] M.C. Cross and P.C. Hohenberg, Rev. Mod. Phys. **65**, 851 (1993).

[16] L. Keefe, Phys. Lett. A **140**, 317 (1989).

[17] W. Press, S. Teukolsky, W. Vetterling, and B. Flannery, *Numerical Recipes in C*, 2nd ed. (Cambridge University Press, Cambridge, 1994).

[18] The existence of an attractor for the Ginzburg-Landau equation was shown by A. Mielke, Nonlinearity **10**, 199 (1997).

[19] The remaining additive constants for both lines are of the order of 1. We calculated the slopes for system lengths $L \geqslant 30 \gg 1$ and therefore the constants can be neglected in the relations for D_L and N.

[20] The fluctuation of Nl/L for large widths l are related to the jumps that occur when the number N of coupling signals increases while increasing the system length L. This effect disappears when the width l is much smaller than L. For example, the jump in Nl/L by incrementing N is still 4% for a width of $l=8$ and a length of $L=200$.

[21] J. Goodwin, R. Brown, and L. Junge, e-print xxx.lanl.gov/abs/chao-dyn/9811002.